

Comparison of Photo- and EB-initiated Polymerizations Based on Equivalent Initiation Energy

Sage M. Schissel, Nicole Kloepfer, and Julie L. P. Jessop
Department of Chemical & Biochemical Engineering, University of Iowa
Iowa City, IA

Abstract

In this study, a protocol was developed to investigate photo- and EB-polymerized films of equivalent initiation energies. This protocol was then applied to a series of monomers to characterize the impact of the initiation mechanism. Raman spectroscopy was used to determine differences in polymer conversion. Monomer chemistry was shown to be a key variable in the comparison of the two initiation mechanisms.

Introduction

Because of the similarity in applications and advantages of these forms of radiation polymerization, the distinction between EB polymerization and photopolymerization is often blurred. Consequently, it is assumed that the polymers produced by each of the two methods are also indistinguishable. Yet, EB polymerization and photopolymerization differ in multiple ways, and previous studies have demonstrated so by comparing their respective polymers.¹⁻³

EB polymerization and photopolymerization differ most notably (on a kinetic scale) in the initiation mechanism. In photopolymerization, specifically free-radical photopolymerization, a photoinitiator (I) decomposes upon exposure to light ($h\nu$) into radicals (R^\bullet), which can then, through the addition of a monomer (M), form the beginning of a propagating polymer chain (M^\bullet) (Equation 1).⁴



In contrast, EB free-radical polymerization does not require an initiator. The accelerated electrons (e^-) are more energetic than the photons of visible/ultraviolet light and, as such, are able to homolytically cleave the bonds of monomer molecules to create the necessary radicals (Equation 2).^{5,6}



This alteration in the initiation mechanism can have far-reaching effects; prominent among them is the increase in cross-linking due to the indiscriminate nature of the electrons. Formation of radicals is a controlled process in photopolymerization, but in EB polymerization, an accelerated

electron can theoretically break any bond it encounters as long as its energy is greater than that required to break the bond.

By comparing EB- and photo-cured polymers, the impact of the initiation mechanism on the polymerization and resulting polymer can be distinguished, due to the remaining polymer mechanisms (propagation and termination) being identical. In addition, through this comparison, photopolymerization can serve as a benchmark for EB studies. EB polymerization is difficult to characterize because of the harsh nature of the accelerated electrons and need for radiation shielding; comparison to the well-developed field of photopolymerization would give insight into such aspects as reaction kinetics, which can only be indirectly measured in EB polymerization.

However, complicating a direct comparison between photo- and EB-initiated polymerization is another difference between the two – energy units. EB dose is measured in kilogray or megarads, with base units of J/g. In contrast, light exposure is measured in J/cm². These units are a reflection of energy deposition for each method of radiation. Light through a film is governed by the Beer-Lambert law: its greatest energy is always at the film surface, and therefore its energy unit is a surface measurement. EB dose as a function of film depth is more complex. It is modeled using Monte Carlo simulations, is affected by film density, and, as such, its energy unit is three-dimensional in nature. In order to obtain a quantitative comparison of the two polymerization methods, the initiation energies must be equal.

In this study, a protocol was developed to investigate photo- and EB-polymerized films of equivalent initiation energies. This protocol was then applied to a series of five acrylate monomers, chosen to characterize the impact of the initiation mechanism. Raman spectroscopy was used to determine differences in polymer conversion.

Experimental

Materials

A series of five monomers was chosen to investigate the impact of initiation mechanism: phenyl acrylate (PA, MP Biomedicals), benzyl acrylate (BA, MP Biomedicals), 2-phenylethyl acrylate (PEA, Polysciences), 2-phenoxyethyl acrylate (POEA, TCI America), and 2-hydroxy-3-phenoxypropyl acrylate (HPOPA, Sartomer) (Figure 1).

An aliphatic urethane diacrylate oligomer, Ebecryl 8807 (proprietary structure, Allnex), was added to each monomer to improve the film properties of the samples. To each monomer/oligomer formulation, the Type 1 photoinitiator 2,2-dimethoxy-2-phenylacetophenone (DMPA, Sigma Aldrich, Figure 1) was added for the photopolymerization reactions. No initiator was used in EB-initiated polymerizations. All materials were used as received and stored at room temperature.

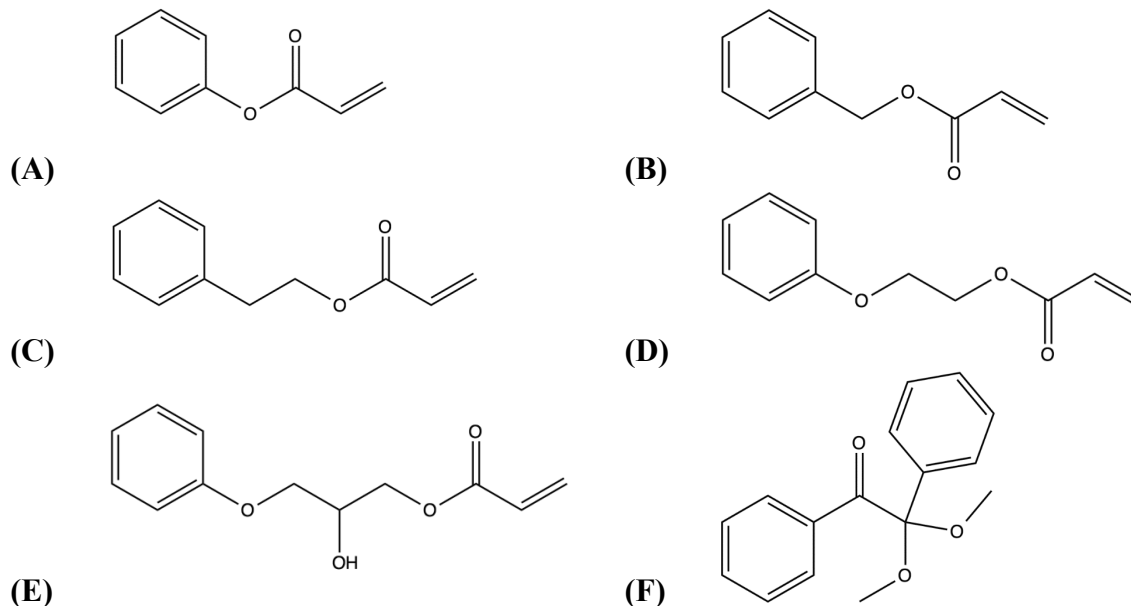


Figure 1. The chemical structures of the 5-monomer series: (A) PA, (B) BA, (C) PEA, (D) POEA, and (E) HPOPA. Also shown is the photoinitiator DMPA (F), which was used in the photopolymerization reactions.

Methods

EB Film Preparation

Each formulation consisted of a 50/50, by weight, mixture of monomer and oligomer. Because of the high viscosity of the oligomer, the formulations were heated to approximately 60°C to allow mixing of the monomer and oligomer. Once heated, formulations were stirred using a drill with a paddle mixer attachment.

Samples for EB curing were prepared by first treating 4 x 3.25 inch glass slides using two coats of Rain-X® 2-in-1 glass cleaner and rain repellent. Next, two layers of lab tape (total thickness ~180 μm) were placed on either side of the glass to be used as spacers. A large droplet, approximately 1 mL, of a formulation was then placed near the top of the slide, between the pieces of tape, and covered with a piece of silicone-coated, 34-μm thick polyethylene terephthalate (PET). A straight edge was drawn across the PET to form a uniform film underneath. The PET cover was used to eliminate the effect of oxygen diffusion in the experiments.

The samples on the glass slides were polymerized by EB irradiation through the PET film using an EB accelerator equipped with a variable-speed, fiberglass carrier web (BroadBeam EP Series, PCT Engineered Systems, Inc.). Three different doses (15, 30, and 60 kGy) and a line speed of 20 ft/min was used to cure the films. Accelerating voltage and N₂ flow rate were held constant at 250 kV and 17 SCFM, respectively. Once polymerized, the films were removed from the glass slides and cut into rectangles measuring 6.25 x 25 mm for characterization. The use of silanized (Rain-X®-treated) glass and silicone-coated PET assisted in the release of the polymer film.

UV Film Preparation

Photo-curable formulations were prepared identical to the EB-curable formulations, with the addition of 0.1 wt% DMPA to the homogenous monomer/oligomer mixture. The formulations were sonicated for 60 minutes to dissolve the photoinitiator. Two pieces of tape (total thickness ~200 μm) were layered, and then a 3 mm diameter hole was punched into the layered tape. The edge of the hole was placed on the edge of a silanized glass microscope slide, and another silanized slide was used to sandwich the tape and create a mold (Figure 2). The formulation was injected into the mold, and Critoseal was used to seal the exposed edge, preventing oxygen diffusion.

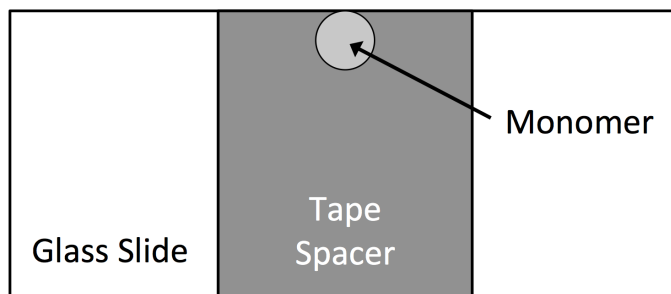


Figure 2. Schematic of the mold used to produce the photopolymerized samples.

An Omnicure® S1000 Ultraviolet/Visible Spot Cure System (Excelitas, 250-450 nm band pass filter) with a 3 mm liquid lightguide was used to polymerize the formulations at ambient temperature. The end of the lightguide was placed directly over the monomer area. Whenever possible, the end of the lightguide was in contact with the glass slide; however, in some instances, the distance was increased to no more than 1 cm to adjust the effective irradiance when the lamp adjustment did not have enough resolution to match the needed value. The effective irradiance was measured by a radiometer (OmniCure, Model No. R2000). After polymerization, samples were removed from the mold and placed on an aluminum Q-panel for Raman characterization.

UV/EB Initiation Energy Comparison

In order to estimate equivalent initiation energies, the energy units of either photopolymerization or EB polymerization needed to be transformed. In this case, the photopolymerization energy units were manipulated to match those of EB polymerization. As illustrated in Equation 3, the units of effective irradiance ($\frac{mW}{cm^2}$) were multiplied by the surface area of the film (cm^2).

$$\frac{mW}{cm^2} * cm^2 * \frac{mJ/s}{mW} * s * \frac{J}{1000 mJ} * \frac{1}{g} = \frac{J}{g} = kGy \quad (3)$$

Then, a conversion factor ($\frac{mJ/s}{mW}$) was used to reduce mW to its base units. Next, the value was multiplied by the exposure time (s) and another conversion factor ($\frac{J}{1000 mJ}$). Finally, the value was divided by the film mass (g), which transformed the units into J/g , or kGy .

Another important aspect to achieving equivalent initiation energies was establishing a consistent energy level throughout the film depth. For the EB-cured films, a voltage of 250 kV was chosen, based on Monte Carlo simulations (Integrated Tiger Series 3 from Oak Ridge National Labs), to ensure a consistent absorbed dose through a 200- μm film (Figure 3).

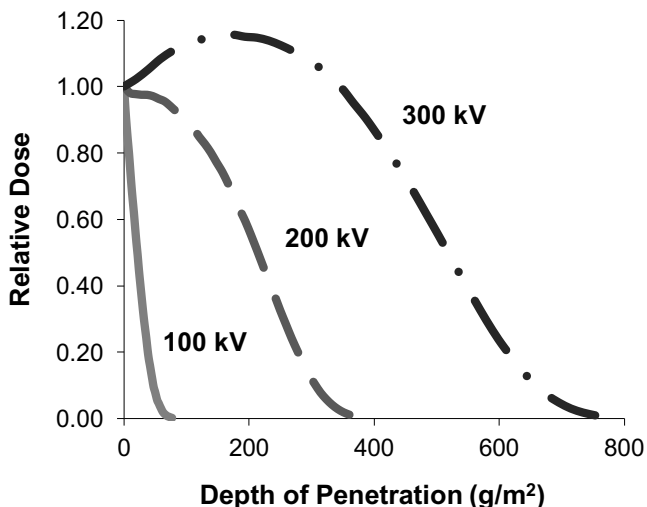


Figure 3. Depth/dose curve for EB polymerization, as predicted by Monte Carlo simulations. With a density of 1 g/cm^3 , the depth of penetration units become micrometers. A voltage of 250 kV was chosen to ensure a consistent dose through a film of $200 \mu\text{m}$.

Similarly, a depth/effective irradiance curve was estimated for the photo-cured films using the model created by Kenning *et al.*, which uses the differential equations governing polychromatic illumination.⁷ The spectral output of the lamp was obtained using an Ocean Optics USB 4000 fiber optic spectrometer. The molar absorptivity of DMPA was collected using an Agilent UV-Visible spectrometer in 1 nm increments.⁸ The photoinitiator concentration was varied to reduce the irradiance gradient through the film depth, and a concentration of 0.1 wt% DMPA was chosen for the photopolymerization studies (Figure 4). By selecting 0.1 wt% as the photoinitiator concentration, the Kenning *et al.* model predicted less than a 15% variance for the equivalent photo-cured films.

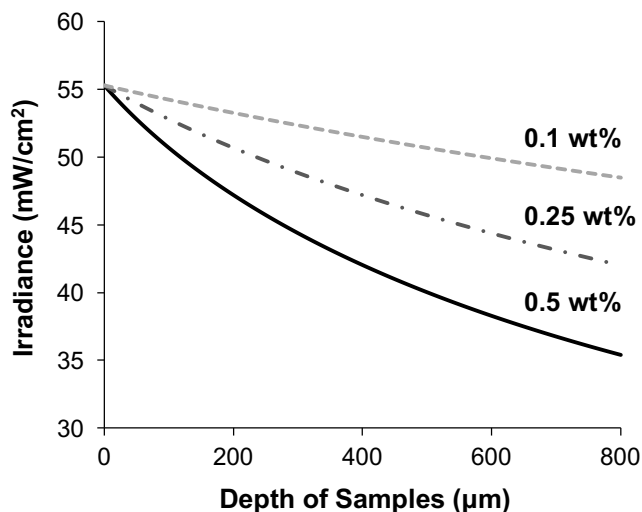


Figure 4. Depth/irradiance curve for photopolymerizations, as predicted by the Kenning *et al.* model, with decreasing concentrations of DMPA. A concentration of 0.1 wt% DMPA was chosen for the photopolymerization studies to reduce the irradiance gradient.

In order to calculate exposure time and effective irradiance, a value of $\left(\frac{cm^2}{g}\right)$ was determined for each monomer/oligomer formulation by photopolymerizing three films, then taking the average of the surface area and mass. Using Equation 3, the effective irradiance needed at the film for each equivalent dose and exposure time was calculated, and then the Kenning *et al.* model was used to determine the effective irradiance setting of the lamp (Table 1).

Table 1. Effective irradiances needed to equal the EB initiation energies for PA (2 s exposure). The irradiances were estimated using Equation 3 and the Kenning *et al.* model.

| Dose (kGy) | Effective Irradiance (mW/cm ²) |
|------------|--|
| 15 | 171 |
| 30 | 341 |
| 60 | 683 |

During a previous study of EB polymerization, the exposure time (dose rate) was shown to greatly influence the polymer properties tested.⁹ Thus, in this study, the same exposure time was used for both EB- and photopolymerized films.

Conversion studies using Raman Spectroscopy

Raman spectroscopy was used to determine conversion of the polymer films. In order to eliminate error from instrumental variations, a reference peak was used. Previous work has established the reaction peak at 1636 cm⁻¹ (indicative of the –C=C– bond in the acrylate moiety) and the reference peak at 1613 cm⁻¹ (indicative of the –C=C– bonds in the phenyl ring) for both photo- and EB polymerization.¹⁰ Conversion, α , was calculated using the following equation:

$$\alpha = \left(1 - \frac{I_{rxn}(P)/I_{ref}(P)}{I_{rxn}(M)/I_{ref}(M)} \right) * 100 \quad (4)$$

where $I_{rxn}(P)$ and $I_{ref}(P)$ are the peak intensities of the reaction and reference peak of the polymer, respectively; $I_{rxn}(M)$ and $I_{ref}(M)$ are the peak intensities of the reaction and reference peak of the monomer.¹¹

Raman spectra of the EB-polymerized films were collected using an optical microscope (DMLP, Leica) connected to a modular research Raman spectrograph (HoloLab 5000R, Kaiser Optical Systems, Inc.) via a 100- μ m collection fiber. A single-mode excitation fiber carried an incident beam of a 785-nm near-infrared laser to the sample through a 10x objective with a numerical aperture of 0.25 and a working distance of 5.8 mm. Laser power at the sample was \sim 10 mW. Spectra were collected with an exposure time of 15 seconds and 3 accumulations. Fifteen monomer spectra were collected and averaged to provide accurate values for $I_{rxn}(M)$ and $I_{ref}(M)$ to use in Equation 4. Three spectra were collected from different areas of each polymer film and averaged to report conversion. Most EB-polymerized films had a standard deviation within \pm 5 percent conversion. Exceptions include: BA 15 kGy-200 ft/min (7%), PA 15 kGy-200 ft/min (27%), PA 30 kGy-100 ft/min (11%), PA 30 kGy-200 ft/min (14%), and PA 60 kGy-100 ft/min (7%).

Raman spectra of the photopolymerized films were collected using a holographic probehead (Mark II, Kaiser Optical Systems, Inc.) with a single-mode excitation fiber and 10x non-contact sampling objective. The incident beam was a 785-nm near-infrared laser with an intensity of \sim 200 mW at the sample. Spectra were collected with an exposure time of 1 second and 3 accumulations. The use of the Raman probehead instead of the microscope for this set of films was the result of the microscope being unavailable during the time period these data were collected; however, the data collected by either attachment are interchangeable. The standard deviation on this set of photopolymerized films was within \pm 5 percent conversion, with only two exceptions: PA 30 kGy-20 ft/min equivalent (7%) and PEA 30 kGy-200 ft/min equivalent (6%).

Results and Discussion

In this study, the effects of the initiation mechanism and monomer chemistry of acrylate formulations on polymer conversion was investigated. Both EB and photopolymerization reactions were studied by Raman spectroscopy to determine the acrylate conversion.

Comparing EB- and photo-cured films with equivalent initiation energies (and exposure times), the EB initiation mechanism produced equal or higher conversions at all studied energy levels (Figure 5). However, the magnitude of the conversion difference between EB- and photo-initiated films appears to be affected both by initiation energy and formulation chemistry.

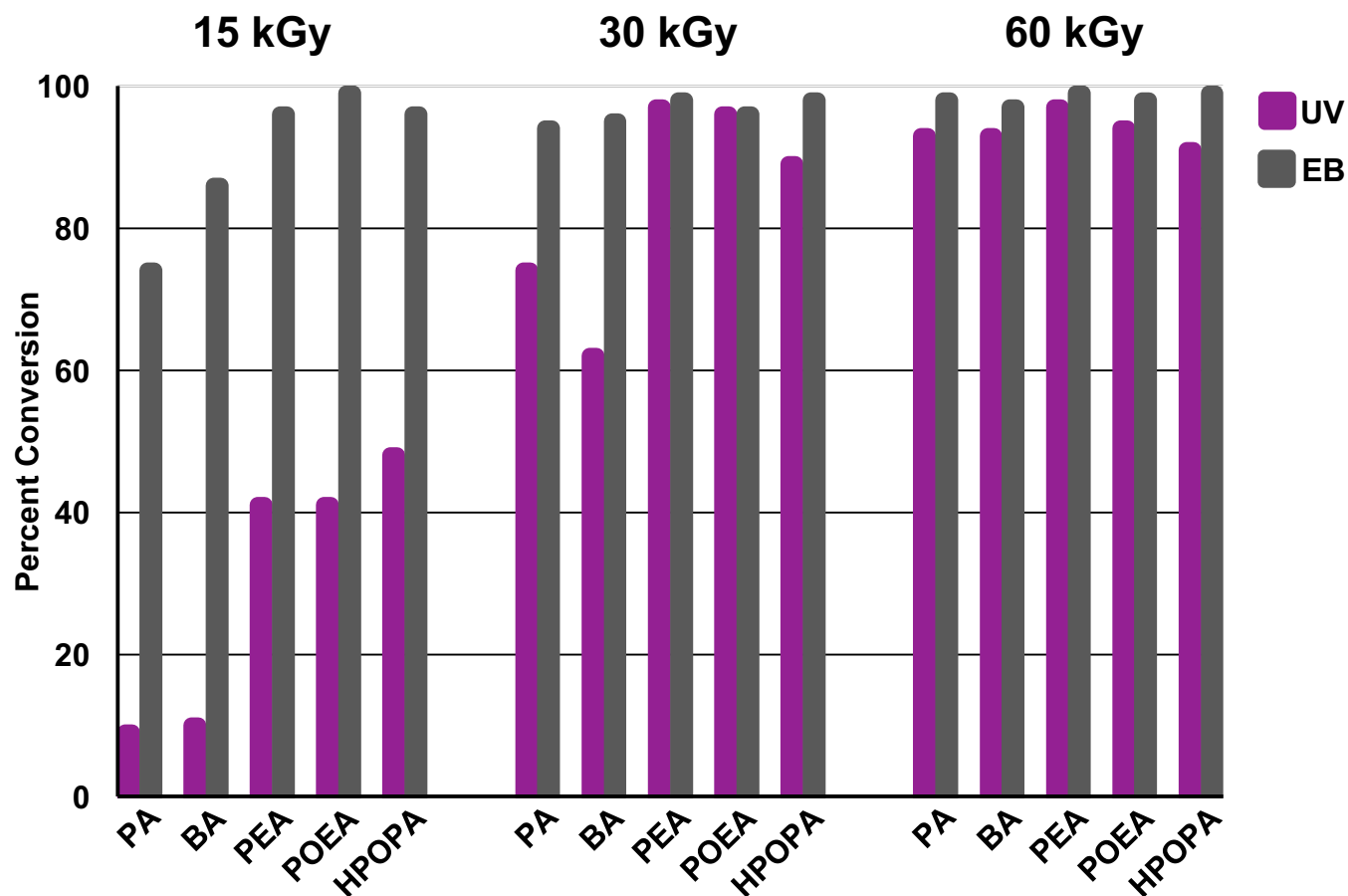


Figure 5. A comparison of UV (purple bars) and EB (gray bars) acrylate conversion for five monomer formulations at three initiation energies. Conversion was measured using Raman spectroscopy.

An increase in the initiation energy, in UV or EB, results in an increase in conversion, which follows the basic principles of free-radical kinetics.⁴ All five monomer formulations follow this trend for both initiation mechanisms. One notable difference, however, is the magnitude of the conversion increase. PA, for example, only achieves 9% conversion at the 15 kGy equivalent exposure energy in UV, which rises to 93% at the 60 kGy equivalent; at the same two energies in EB, the conversion increase is only 74% to 98% (Figure 6). While PA is an extreme case, no monomer formulation initiated by UV at the 15 kGy equivalent reached $\geq 50\%$ conversion, yet no formulation initiated by EB at the same initiation energy had less than 70% conversion.

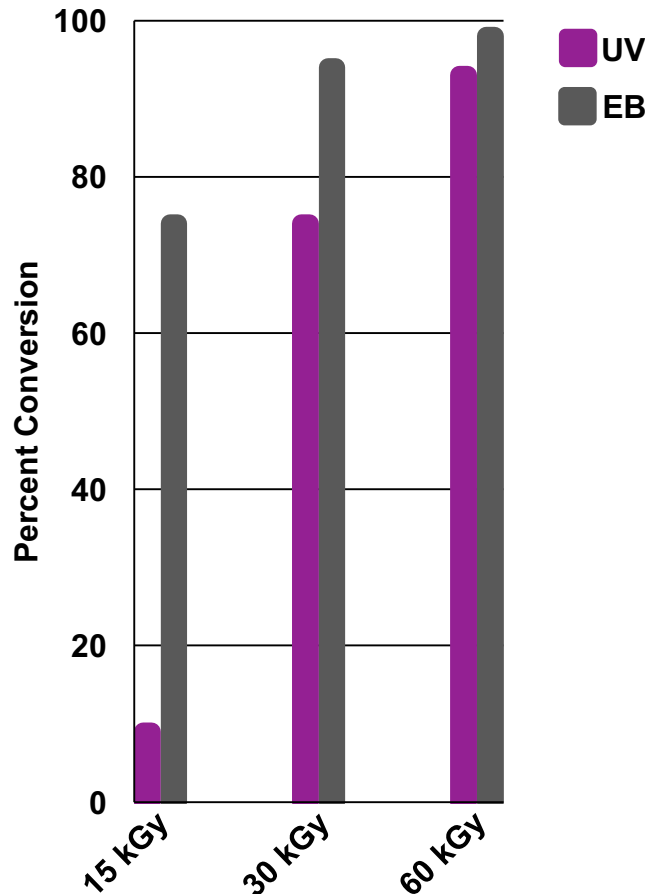


Figure 6. A comparison of UV (purple bars) and EB (gray bars) acrylate conversion for the PA formulations at three initiation energies. Conversion was measured using Raman spectroscopy.

Conversion was also shown to be dependent on formulation chemistry. This dependence is most prominent in the 15 kGy data where conversion levels were not completely saturated (Figure 5). In both the EB- and photo-initiated systems, PA and BA had the lowest conversion levels across the five monomer series. Conversion increases across the series generally from smallest monomer (PA) to largest (HPOPA). Because this trend is evident in both the EB and photopolymerized formulations, it is likely due to a cause independent of the initiation mechanism and inherent to the monomer chemistry.

These conversion differences between the EB and photopolymerized films and their dependence on initiation energy and formulation chemistry may be attributed to differences in the number of propagating radicals, network formation, or both. Despite having equivalent initiation energies, the EB and photopolymerized systems do not necessarily have equivalent concentrations of propagating radicals. In fact, the large differences in conversion between the EB- and photo-initiated systems at 15 kGy support EB having generated more radicals than UV at that initiation energy. The Kenning *et al.* model used to estimate the photo-initiation energy accounts for the quantum yield of the photoinitiator; however, the quantum yield is defined as the fraction of absorbed photons leading to initiator fragmentation, or primary radicals (R^*).⁷ While it is generally assumed that primary radicals react with monomer to become propagating radicals

(M' , Equation 1), at least some primary radicals are quenched by dissolved oxygen, introducing error in the estimation. In EB, not even primary radical concentration is known since the radiation yield G_R , defined as the number of free radicals created per 100 eV absorbed, is unknown.⁶ Even if G_R was known for each of the monomers, the number of side reactions (namely crosslinking reactions) in EB would increase the error in estimating what fraction of primary radicals become propagating radicals. If the concentration of propagating radicals is not equivalent for each radiation, the rate of propagation and termination will be affected and could account for the differences in the conversion.

Differences in network formation may also contribute to the discrepancies in conversion for the two initiation mechanisms. In photopolymerization, network formation is relatively controlled. In the absence of chain transfer, monofunctional acrylates form linear polymers, and multifunctional acrylates form branched or cross-linked networks. EB polymerization, in contrast, is known for its side reactions (caused by the indiscriminate nature of accelerated electrons breaking bonds), which can produce a cross-linked network even with monofunctional monomers (Equation 2). If the EB-cured films produce a more heavily cross-linked network, especially earlier in the reaction, termination by trapping (monomolecular termination) may become dominant. Monomolecular termination changes the rate of termination's dependence on radical concentration to first order, therefore reducing the rate of termination relative to the rate of propagation and promoting conversion.⁴

Conclusions

A protocol was developed to estimate equivalent initiation energies between EB and photopolymerization. This protocol relies primarily on the Kenning *et al.* model to estimate the absorbed photon energy and is straightforward to implement. By establishing a non-arbitrary basis on which to compare EB and photopolymerization, the more developed field of photopolymerization can be used as an effective benchmark to evaluate the results in EB polymerization.

This protocol was also used to compare EB-initiated films to photo-initiated films of the same initiation energy and equivalent exposure time. The photopolymerized films were shown to have equal or lower conversions, and they followed the monomer chemistry trends established in the EB films. Differences in the magnitude of conversion were hypothesized to be a result of unequal radical concentrations and/or changes to the polymer network caused by the initiation mechanism. Future work will use the protocol to test these hypotheses.

Acknowledgements

This material is based upon work supported by the National Science Foundation under Grant No. 1264622 and The University of Iowa Mathematical & Physical Sciences Funding Program.

References

- (1) Patacz, C.; Coqueret, X.; Decker, C. Electron-Beam Initiated Polymerization of Acrylate Compositions 3: Compared Reactivity of Hexanediol and Tripropyleneglycol Diarylates Under UV or EB Initiation. *Radiation Physics and Chemistry* **2001**, *62*, 403–410.
- (2) Glauser, T.; Johansson, M.; Hult, A. A Comparison of Radiation and Thermal Curing of Thick Composites. *Macromolecular Materials and Engineering* **2000**, *274*, 25–30.
- (3) Batten, R. J.; Davidson, R. S.; Wilkinson, S. A. Radiation Curing of an Epoxy-Acrylate-6,7-Epoxy-3,7-Dimethyloctyl Acrylate. *Journal of Photochemistry and Photobiology A: Chemistry* **1991**, *58* (1), 115–122.
- (4) Odian, G. *Principles of Polymerization*, 4 ed.; John Wiley and Sons, Inc., **2004**.
- (5) Richter, K. B. *Pulsed Electron Beam Curing of Polymer Coatings*. **2007**, 1–246.
- (6) *Radiation Curing: Science and Technology*, 1st ed.; Pappas, S. P., Ed.; Springer Science & Business Media: New York, **1992**.
- (7) Kenning, N. S.; Kriks, D.; El-Maazawi, M.; Scranton, A. Spatial and Temporal Evolution of the Photoinitiation Rate for Thick Polymer Systems Illuminated with Polychromatic Light. *Polym. Int.* **2006**, *55* (9), 994–1006.
- (8) Kenning, N. L. Spatial and Temporal Evolution of the Photoinitiation Rate in Thick Polymer Systems, **2006**, pp 1–163.
- (9) Schissel, S. M.; Lapin, S. C.; Jessop, J. L. P. “Characterization and Prediction of Monomer-based Dose Rate Effects in Electron-beam Polymerization,” *Radiation Physics & Chemistry*, Vol. 141, 2017, 41-49.
- (10) Schissel, S. M.; Lapin, S. C.; Jessop, J. L. P. Internal Reference Validation for EB-Cured Polymer Conversions Measured via Raman Spectroscopy. *RadTech Report* **2014**, No. 4, 46–50.
- (11) Cai, Y.; Jessop, J. L. P. Decreased Oxygen Inhibition in Photopolymerized Acrylate/Epoxy Hybrid Polymer Coatings as Demonstrated by Raman Spectroscopy. *Polymer* **2006**, *47* (19), 6560–6566.